OPTIMIZATION OF NON-SYMMETRIC COMPOSITE PANELS USING FAST ANALYSIS TECHNIQUES

Riccardo Vescovini and Chiara Bisagni[*]

Department of Aerospace Science and Technology, Politecnico di Milano
Via La Masa 34, 20156, Milano, Italy
Email: riccardo.vescovini@polimi.it, chiara.bisagni@polimi.it, web page: http://www.aero.polimi.it

ABSTRACT

A semi-analytical approach is presented for the optimization of laminated panels with nonsymmetric lay-ups, and with the possibility of introducing requirements on the buckling load, the postbuckling response and the eigenfrequencies. The design strategy relies on the combined use of semi-analytical techniques for the structural analysis and genetic algorithms for the optimization. The structural analysis is performed with a highly efficient code based on thin plate theory, where the problem is formulated in terms of Airy stress function and out of plane displacement, expanded using trigonometric series. The solution of two distinct eigenvalue problems is performed to determine eigenfrequencies and buckling load, while an arc-length method is adopted for the postbuckling computation. The genetic algorithm is implemented by using proper alphabet cardinalities to handle different steps for the angles of orientation, while specific mutation operators are used to guarantee good reliability of the optimization. To show the potentialities of the proposed optimization toolbox, two examples are presented regarding the design of balanced non-symmetric laminates subjected to linear and nonlinear constraints. The accuracy of the analytical predictions is demonstrated by comparison with finite element results.

1   INTRODUCTION

In the past years, many efforts have been directed towards the development of analytical and semi-analytical methods for the fast analysis of composite panels [1]. In most cases, the methods have focused on symmetrically layered structures, thus avoiding the coupling between the in plane and out of plane behaviour of the panel. Relatively few works have dealt with non-symmetric lay-ups. Similarly, several design optimization procedure have been developed by restricting the design space to the case of symmetric lay-ups. Examples are found in two works of the authors [2, 3], where analytical tools are coupled with genetic algorithms, and symmetric lay-ups are assumed. In order to fully exploit the tailoring opportunities offered by composite materials, novel analysis tools are needed to handle more generic lay-up configurations. In this context, closed-form solution are a useful mean to guarantee computational effectiveness, which is particularly useful when dealing with optimization procedures. However, the complexity of the mechanical couplings characterizing the response of generally layered panels often requires the introduction of several simplifying assumptions.

An early work of Chandra [4] presents a single-term solution to analyse unsymmetric panels and is restricted to the case of axially compressed cross-ply configurations. The Rayleigh-Ritz method is adopted by Dano and Hyer [5] to study the response of non-symmetric panels during the cooling from the cure temperature. More recently, closed-form solutions were derived by Diaconu and Weaver [6] using a single-term approximation to represent the out of plane displacement and considering compression load. Nie and Liu [7] extended the formulation to account for shear loads and elastic restraints. Both in Refs. [6] and [7], the approach is valid for infinitely long panels only, and any mode change or snap cannot be accounted for. Many of the restrictions necessary to derive closed-form solution can be relaxed by adopting multiple-series solutions. In these cases, the equations can be obtained analytically, but the solution is computed numerically.

*Currently at TU-Delft, Faculty of Aerospace Engineering, Kluyverweg 1, 2629 HS Delft, The Netherlands.

An example is found in the work of Zhang and Matthews [8], where the Airy stress function and the out of plane displacement are approximated with sine terms or beam eigenfunctions. Zhang at al. [9] proposed a formulation based on Karman-Reissner plate theory and asymptotic series solution to study the buckling and the postbuckling response of non-symmetric plates. In both cases, the governing equations regard the out of plane equilibrium and the strain compatibility. The total number of degrees of freedom is still smaller if compared to finite elements, but significantly higher with respect to closed-form solutions.

The present work aims to fill the gap between closed-form solutions and semi-analytical approaches by presenting a highly efficient solution based on multiple degrees of freedom, but characterized by analysis time comparable to closed-form solutions. The approach, which is developed for finite length non-symmetric plates and subjected to generic boundary and loading conditions of compression, is adopted in the context of a design optimization based on genetic algorithms with linear and nonlinear constraints. In particular, buckling, eigenfrequency and postbuckling response are accounted for.

2   ANALYTICAL MODEL

The analysis tool is based on thin plate assumptions and Classical Lamination Theory (CLT). Flat rectangular panels are considered, with the four edges elastically restrained against the rotation. The edges can be restrained with a torsion spring of arbitrary stiffness, thus defining any intermediate condition between clamped and simply-supported conditions. Furthermore, it is assumed that the four edges are free to move along their normal direction, but are forced to remain straight. This latest assumption is introduced to account for the presence of the surrounding structure. Loading conditions of compression are considered. A Cartesian coordinate system is taken over the panel midsurface with the x-axis directed along the longitudinal direction, the y-axis along the transverse direction and the z-axis to define a right-handed system. It is here assumed that the panel is part of a larger structure, as in the case of aircraft panels, which are assembled in repeating units. A sketch of the panel is reported in Figure 1.
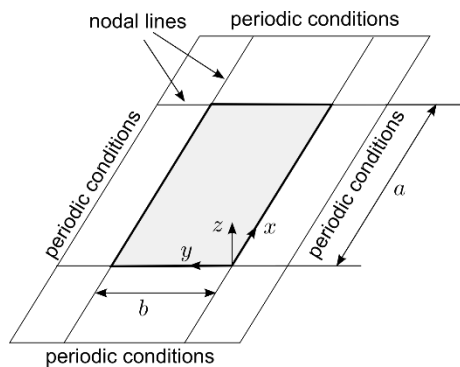

Figure 1: Panel geometry and reference system.

The laminate is layered with an arbitrary number of plies, not necessarily stacked to guarantee the symmetry with respect to the midplane of the panel. The only assumption here introduced is that one of balanced laminate, meaning that the presence of a ply at $+\theta$ requires the presence of a ply at $-\theta$. The semi-inverse constitutive law of the laminate is:

$$\begin{Bmatrix} \boldsymbol{\xi} \\ \mathbf{M} \end{Bmatrix} = \begin{bmatrix} \mathbf{a} & \mathbf{e} \\ -\mathbf{e}^{\mathrm{T}} & \mathbf{d} \end{bmatrix} \begin{Bmatrix} \mathbf{N} \\ \mathbf{k} \end{Bmatrix} \tag{1}$$

where $\mathbf{N}$ and $\mathbf{M}$ are the force and moment resultant along the thickness, while $\boldsymbol{\xi}$ and $\mathbf{k}$ are the membrane strains and the curvatures, respectively. The matrices $\mathbf{a}$, $\mathbf{d}$, $\mathbf{e}$ of Eq. (1) are related to the CLT matrices through the relations $\mathbf{a} = \mathbf{A}^{-1}$, $\mathbf{e} = -\mathbf{A}^{-1}\mathbf{B}$, $\mathbf{d} = \mathbf{D} - \mathbf{B}\mathbf{A}^{-1}\mathbf{B}$. Under the assumption of balanced laminate and using the Voigt notation, the only null terms of Eq. (1) are a_{16} and a_{26}.

2.1   Variational principle

The postbuckling problem is developed within a variational framework, and is based on the minimum potential energy principle. The buckling equations, as well as those regarding the free vibrations, can be derived from the linearization of the nonlinear approach. The total potential energy of the laminate is:

$$\Pi = \Pi_m + \Pi_b + \Pi_k - V_c \tag{2}$$

where Π_m denotes the contribution due to the membrane stretching, Π_b is the bending energy and Π_k the strain energy stored in the elastic restraints. The term V_c is the potentials of the external compressive loads. The strategy here proposed relies on the so-called *w-F* approach, where the unknowns of the problem are the out of plane deflection w and the Airy stress function F. Referring to Eq. (2), the equilibrium configuration is obtained by solution of the following constrained minimization problem:

$$\delta\Pi = 0$$
$$\text{subjected to } L_L(F, w) + \frac{1}{2}L_{NL}(w, w + 2w_0) = 0 \tag{3}$$

where w_0 defines the initial imperfection. The constraint of Eq. (3) is the compatibility requirement, expressed in terms of the linear and nonlinear operators L_L and L_{NL}, whose expressions are:

$$L_L(F, w) = a_{11}F_{,yyyy} + (2a_{12} + a_{66})F_{,xxyy} + a_{22}F_{,xxxx} - e_{21}w_{,xxxx} - (e_{11} + e_{22} -$$
$$2e_{66})w_{,xxyy} - e_{12}w_{,yyyy} - (2e_{26} - e_{61})w_{,xxxy} - (2e_{16} - e_{62})w_{,xyyy} \tag{4}$$

$$L_{NL}(w, w + 2w_0) = w_{,xx}(w + 2w_0)_{,yy} - 2w_{,xy}(w + 2w_0)_{,xy} + w_{,yy}(w + 2w_0)_{,xx} \tag{5}$$

The comma followed by an index denotes differentiation with respect to that index. The membrane and the bending contributions, expressed in terms of Airy stress function and out of plane displacement, are:

$$\Pi_m = \frac{1}{2}\int_{-a/2}^{3a/2}\int_{-b/2}^{3b/2}\left(a_{11}F_{,yy}^2 + 2a_{12}F_{,xx}F_{,yy} + a_{22}F_{,xx}^2 + a_{66}F_{,xy}^2\right)dxdy \tag{6}$$

$$\Pi_b = \frac{1}{2}\int_{-a/2}^{3a/2}\int_{-b/2}^{3b/2}\left(d_{11}w_{,xx}^2 + 2d_{12}w_{,xx}w_{,yy} + d_{22}w_{,yy}^2 + 2d_{16}w_{,xx}w_{,xy} + 2d_{26}w_{,yy}w_{,xy}\right.$$
$$\left. + 4d_{66}w_{,xy}^2\right)dxdy \tag{7}$$

The terms a_{ik} and d_{ik} are the components of the constitutive law of the in plane compliance of the laminate and the so-called reduced bending stiffness, respectively. It is worth observing that the coupling terms due to the non-symmetry of the laminate enter in the bending energy expression as the matrix **d** is function of **B**. The potential of the compression load, introduced with a uniform end displacement, is:

$$V_c = 2b\,\bar{N}_x\Delta\bar{U} \tag{8}$$

where $\bar{N}_x$ is the average stress resultant during the loading phase, and $\Delta\bar{U}$ is the average end shortening of the panel, defined as:

$$\Delta\bar{U} = \frac{\bar{N}_x}{2b}\int_{-a/2}^{3a/2}\int_{-b/2}^{3b/2}\left(-\xi_x + \frac{1}{2}w_{,x}^2 + w_{0,x}w_{,y} + w_{0,y}w_{,x}\right)dx\,dy \tag{9}$$

The essential boundary conditions of the problem are expressed as:

$$\begin{cases} w = 0 & \text{at}\quad x = 0, a\ \ y = 0, b \\ \Delta U = \text{const} & \text{at}\quad x = 0, a \\ \Delta V = \text{const} & \text{at}\quad y = 0, b \end{cases} \tag{10}$$

It is worth noting that the two conditions regarding the in plane displacement of the edges are not exactly met within the approach here proposed. However, they are satisfied in a weak form, leading, as demonstrated in the next, to accurate results.

2.2   Ritz solution

The stationarity condition of Eq. (3) is imposed referring to the method of Ritz. The out of plane displacement and the initial imperfections are approximated with a double series of sine terms as:

$$w = \sum_{mn}^{RS} q_{mn} \sin\frac{m\pi x}{a} \sin\frac{n\pi y}{b} = \mathbf{N}^w\mathbf{q}; \qquad w_0 = \sum_{mn}^{RS} q_{mn}^0 \sin\frac{m\pi x}{a} \sin\frac{n\pi y}{b} = \mathbf{N}^w\mathbf{q}^0 \qquad (11)$$

The unknown amplitudes q_{mn} of Eq. (11) are collected in the column vector $\mathbf{q}$ of dimensions R×S defined as $\mathbf{q} = \{q_{11} \dots q_{1S}\ q_{21} \dots q_{2S} \dots\dots \dots q_{RS}\}^T$, and the matrix of the shape functions $\mathbf{N}^w$ is defined accordingly. The same strategy is adopted for the initial imperfection, the only difference being the fact that the amplitudes $\mathbf{q}^0$ are known a priori to achieve the desired geometric imperfection shape. The expansion of Eq. (11) guarantees that the first of the three essential boundary conditions of Eq. (10) is identically satisfied.

To ensure the respect of the compatibility requirement of Eq. (3), the Airy stress function is expanded as the sum of five contributions:

$$F(x, y) = \frac{1}{2}\bar{N}_x y^2 + \bar{N}_{xy} xy + F_{NL}(x, y) + G(x, y) + H(x, y) \qquad (12)$$

where the first two terms are responsible for the uniform stress distribution over the panel, while the functions F_{NL}, G and H describe the stress redistribution due to the panel deflection. In particular, the term F_{NL} is relative to the postbuckling nonlinear stress redistribution, and its expression is:

$$F_{NL}(x, y) = \sum_{mn=0}^{2R2S} f_{mn} \cos\frac{m\pi x}{a} \cos\frac{n\pi y}{b} = \mathbf{N}^{NL}\mathbf{f} \qquad (13)$$

The vector of amplitudes $\mathbf{f}$ can be expressed in terms of $\mathbf{q}$ by substitution of Eqs. (11) and (13) into the compatibility requirement of Eq. (3). It can be demonstrated that the generic coefficient f_i is a quadratic function of the deflection amplitudes $\mathbf{q}$, and is obtained by:

$$f_i = \mathbf{q}^T\mathbf{B}_i^{sym}\left(\frac{1}{2}\mathbf{q} + \mathbf{q}^0\right) \qquad (14)$$

where $\mathbf{B}_i^{sym} = \mathbf{B}_i + \mathbf{B}_i^T$, and the term $\mathbf{B}_i$ is a matrix of scalar coefficients, built according to the approach reported in Refs. [10, 11].

The functions G and H of Eq. (12) describe the stress distribution due to the linear coupling between the in plane and out of plane response of the plate. Their expression is sought in the form:

$$G(x, y) = \sum_{mn=1}^{RS} g_{mn} \cos\frac{m\pi x}{a} \cos\frac{n\pi y}{b} = \mathbf{N}^g\mathbf{g} = \mathbf{N}^g \text{ diag}[\mathbf{b}^g]\mathbf{q}$$

$$H(x, y) = \sum_{mn=1}^{RS} h_{mn} \sin\frac{m\pi x}{a} \sin\frac{n\pi y}{b} = \mathbf{N}^h\mathbf{g} = \mathbf{N}^h \text{ diag}[\mathbf{b}^h]\mathbf{q} \qquad (15)$$

where the relation between the amplitudes g_{mn}, h_{mn} and $q_{mn}$is given by the vectors $\mathbf{b}^g$ and $\mathbf{b}^h$, whose expression is obtained by substitution of Eq. (15) into the compatibility equation. The generic component b_i^g of the vector $\mathbf{b}^g$ is:

$$b_i^g = \frac{(2e_{26} - e_{61})\left(\frac{m}{a}\right)^3\frac{n}{b} + (2e_{16} - e_{62})\frac{m}{a}\left(\frac{n}{b}\right)^3}{a_{11}\left(\frac{n}{b}\right)^4 + (2a_{12} + a_{66})\left(\frac{mn}{ab}\right)^2 + a_{22}\left(\frac{m}{a}\right)^4} \qquad (16)$$

Similarly, the vector $\mathbf{b}^h$ has components:

$$b_i^h = \frac{e_{21}\left(\frac{m}{a}\right)^4 + (e_{11} + e_{22} - 2e_{66})\left(\frac{mn}{ab}\right)^2 + e_{12}\left(\frac{n}{b}\right)^4}{a_{11}\left(\frac{n}{b}\right)^4 + (2a_{12} + a_{66})\left(\frac{mn}{ab}\right)^2 + a_{22}\left(\frac{m}{a}\right)^4} \qquad (17)$$

As observed in Eqs. (13)-(17), the unknown amplitudes of the Airy stress function can be expressed in terms of the amplitudes $\mathbf{q}$, which are the only unknown of the problem. After substitution of Eqs. (13) and (15) into (6), the membrane energy can be written as the sum of three contributions:

$$\Pi_m = \Pi_m^{lin} + \Pi_m^{nl,ff} + \Pi_m^{nl,fg} \qquad (18)$$

The first term of Eq. (18) is quadratic in $\mathbf{q}$ and is null for symmetric panels. The second and the third terms are quartic and cubic in $\mathbf{q}$, respectively. After collecting the coefficients obtained from the analytical integration of the membrane energy in the matrices $\boldsymbol{\alpha}^{gg}$, $\boldsymbol{\alpha}^{hh}$ and $\boldsymbol{\alpha}^{fg}$, it is obtained:

$$\Pi_m^{lin} = \frac{1}{2}\mathbf{g}^T\boldsymbol{\alpha}^{gg}\mathbf{g} + \frac{1}{2}\mathbf{h}^T\boldsymbol{\alpha}^{hh}\mathbf{h}; \qquad \Pi_m^{nl,ff} = \frac{1}{2}\mathbf{f}^T\boldsymbol{\alpha}^{ff}\mathbf{f}; \qquad \Pi_m^{nl,fg} = \frac{1}{2}\mathbf{f}^T\boldsymbol{\alpha}^{fg}\mathbf{g} \tag{19}$$

The bending energy is directly computed by substitution of Eq. (11) into Eq. (7), and is written as:

$$\widetilde{\Pi}_b = \Pi_b + \Pi_k = \frac{1}{2}\mathbf{q}^T(\mathbf{K}_b + \mathbf{K}_k)\mathbf{q} = \frac{1}{2}\mathbf{q}^T\widetilde{\mathbf{K}}_b\mathbf{q} \tag{20}$$

where $\widetilde{\mathbf{K}}_b$ is the reduced bending stiffness matrix, including also the contribution due to the springs. Regarding the contribution of the applied loads, it is obtained by substitution of Eq. (11) into (8), and is written as:

$$V_c = \overline{N}_x^2 \, ab \, a_{11} + \frac{1}{2}\mathbf{q}^T\mathbf{K}_c(\mathbf{q} + 2\mathbf{q}^0) \tag{21}$$

The matrices $\mathbf{K}_c$ and $\mathbf{K}_s$ collect the numerical coefficients obtained from the closed-form integration of the integrals involved in the expressions of the potential of the external loads.

2.3 Postbuckling equations

The nonlinear equations governing the postbuckling response of the panel are derived following the approach discussed in Refs. [10, 11], where a perturbation arc length approach is implemented. The main advantage of this solution scheme relies in its robustness to capture mode changes or snaps. This feature is particularly interesting in the context of an optimization procedure, where it becomes mandatory to guarantee that each of the structural analysis terminates without convergence issues. The set of nonlinear equations governing the postbuckling behaviour of the panel are derived in rate form as:

$$\frac{\partial\Pi_{,\eta}}{\partial\mathbf{q}} = \mathbf{K}\mathbf{q}_{,\eta} + \mathbf{s}\Lambda_{,\eta} = \mathbf{0} \tag{22}$$

where Λ and η are the load and the rate parameters, respectively. The first term in the right hand side of Eq. (22), is the tangent stiffness matrix, while the second contribution is the incremental load vector, which are defined as:

$$\mathbf{K} = \frac{\partial^2\Pi}{\partial\mathbf{q}^2} \qquad \mathbf{s} = \frac{\partial\Pi}{\partial\mathbf{q}\,\partial\Lambda} \tag{23}$$

The tangent stiffness matrix $\mathbf{K}$ is obtained as the sum of two contributions, a linear term independent on the configuration, and a nonlinear term which is function of the current deformation. The matrix is so re-written as:

$$\mathbf{K} = \mathbf{K}^{lin} + \mathbf{K}_m^{nl}(\mathbf{q}) \tag{24}$$

where the linear contribution is derived from:

$$\begin{aligned}\mathbf{K}^{lin} &= \frac{\partial^2\left(\widetilde{\Pi}_b + \Pi_m^{lin} + V_c + V_s\right)}{\partial\mathbf{q}^2}\\ &= \widetilde{\mathbf{K}}_b + \mathbf{B}^{g^T}\boldsymbol{\alpha}^{gg}\mathbf{B}^g + \mathbf{B}^{h^T}\boldsymbol{\alpha}^{hh}\mathbf{B}^h + \Lambda(\mathbf{K}_c + \mathbf{K}_s)\end{aligned} \tag{25}$$

The second contribution to the tangent stiffness matrix is due to the nonlinear terms of the membrane energy, as observed in Eqs. (18) and Eq. (19). The two terms are written as:

$$\mathbf{K}_m^{nl} = \mathbf{K}_m^{nl,ff} + \mathbf{K}_m^{nl,fg} \tag{26}$$

where $\mathbf{K}_m^{nl,ff}$ is obtained by recalling the second of (19). In particular, it is:

$$\mathbf{K}_m^{nl,ff} = \frac{\partial^2\Pi_m^{nl,ff}}{\partial\mathbf{q}^2} = \sum \frac{\partial f_i}{\partial\mathbf{q}}\frac{\partial^2\Pi_m^{nl,ff}}{\partial f_i\,\partial f_j}\frac{\partial f_j}{\partial\mathbf{q}} + \sum \frac{\partial\Pi_m^{nl,ff}}{\partial f_i}\frac{\partial f_i}{\partial\mathbf{q}^2} \tag{27}$$

From the expressions of Eqs. (14) and (19), the expression of the nonlinear stiffness due the membrane energy is obtained as:

$$\mathbf{K}_m^{nl,ff} = \sum_{i=0}^{2R2S} \mathbf{B}_i^{sym}(\mathbf{q} + \mathbf{q}^0)\alpha_{ij}^{ff}(\mathbf{q} + \mathbf{q}^0)^T\mathbf{B}_j^{sym} + v_i\mathbf{B}_i^{sym} \tag{28}$$

where the term v_i is the i-th component of the vector $\mathbf{v}$, obtained as:

$$\mathbf{v} = \boldsymbol{\alpha}^{ff}\mathbf{f} \tag{29}$$

and the components of the vector $\mathbf{f}$ are obtained according to Eq. (14).The second contribution to the nonlinear part of the tangent stiffness matrix regards the coupling between the functions F and G, and is derived as:

$$\mathbf{K}_m^{nl,fg} = \frac{\partial^2 \Pi_m^{nl,fg}}{\partial \mathbf{q}^2} = \sum_{i=0}^{2R2S}\sum_j^{RS}\frac{\partial f_i}{\partial \mathbf{q}}\frac{\partial^2 \Pi_m^{nl,fg}}{\partial f_i \partial g_j}\frac{\partial g_j}{\partial \mathbf{q}} + \frac{\partial g_i}{\partial \mathbf{q}}\frac{\partial^2 \Pi_m^{nl,fg}}{\partial g_i \partial f_j}\frac{\partial f_j}{\partial \mathbf{q}} + \sum_{i=0}^{2R2S}\frac{\partial \Pi_m^{nl,fg}}{\partial f_i}\frac{\partial f_i}{\partial \mathbf{q}^2}$$
$$= \widetilde{\mathbf{K}} + \widetilde{\mathbf{K}}^T + w_i\mathbf{B}_i^{sym} \tag{30}$$

where the matrix $\widetilde{\mathbf{K}}$ is defined as:

$$\widetilde{\mathbf{K}} = \sum_{i=0}^{2R2S} \mathbf{B}_i^{sym}(\mathbf{q} + \mathbf{q}^0)\alpha_{ij}^{fg}\tilde{\mathbf{b}}_j^g \tag{31}$$

The row vector $\tilde{\mathbf{b}}_j^g$ is the j-th row of the matrix $\text{diag}[\mathbf{b}^g]$, and the term w_i of Eq. (30) is the i-th component of the vector $\mathbf{w}$, obtained as:

$$\mathbf{w} = \boldsymbol{\alpha}^{fg}\mathbf{B}^g\mathbf{q} \tag{32}$$

The derivation of the incremental load vector $\mathbf{s}$ is straightforward, and is obtained as:

$$\mathbf{s} = \frac{\partial V_c}{\partial \mathbf{q}\,\partial \Lambda} = \Lambda\boldsymbol{\alpha}_c\,(\mathbf{q} + \mathbf{q}^0) \tag{33}$$

2.4 Buckling equations

The buckling equations can be derived from the linearization of the nonlinear, discrete equations of Eq. (22). In particular, the buckling eigenvalue problem is obtained by setting to zero the incremental load vector $\mathbf{s}$, and by considering null initial imperfections, i.e. $\mathbf{s} = \mathbf{0}$ and $\mathbf{q}^0 = \mathbf{0}$.
Moreover, the approximation of null prebuckling deflections is introduced, i.e. $\mathbf{q} = \mathbf{0}$, although for a non-symmetric laminate this condition is not exactly met due to the coupled in plane and out of plane response. Under the above mentioned assumptions, the problem is reduced to a standard linear eigenvalue problem in the form:

$$\left[\left(\widetilde{\mathbf{K}}_b + \mathbf{K}_m^{lin}\right) + \lambda\mathbf{K}_c\right]\mathbf{q} = \mathbf{0} \tag{34}$$

where the contributions to the stiffness matrix and the loading matrix are the same derived in Eq. (25).

2.5 Eigenfrequency equations

The equations governing the linear free vibrations of the panel are derived by introducing the Lagrangian L, which is defined as:

$$L = T - (\Pi_m^{lin} - \Pi_b) \tag{35}$$

The second and the third contributions in the right hand side of Eq. (35) are available from Eqs. (19) and (20), while the kinetic energy T is introduced by neglecting the contribution of the in plane inertia as:

$$T = \frac{1}{2}\rho\int_{-a/2}^{3a/2}\int_{-b/2}^{3b/2}\left(\dot{u}_{,x}^2 + \dot{v}_{,x}^2 + w_{,x}^2\right)dxdy \approx \frac{1}{2}\rho\int_{-a/2}^{3a/2}\int_{-b/2}^{3b/2}w_{,x}^2\,dxdy \tag{36}$$

where ρ denotes the density per unit surface of the panel. The solution of the free harmonic motion is sought as follows:

$$w(x, y, t) = w(x, y)e^{i\omega t} \tag{37}$$

After substituting Eq. (37) into Eq. (36) and performing the integrals in closed-form manner, the approximated kinetic energy is derived in terms of the problem unknowns **q**. The discrete equations of the panel free vibrations are finally obtained as a standard eigenvalue problem of dimensions RS×RS in the form:

$$\frac{\partial L}{\partial \mathbf{q}} = \left[-\omega^2 \mathbf{M} + \left(\mathbf{K}_b + \mathbf{K}_m^{lin} \right) \right] \mathbf{q} = \mathbf{0} \tag{38}$$

3   OPTIMIZATION ALGORTHM

The optimization process is here performed with a code based on the standard genetic algorithm (GA) implementation with modifications specifically introduced for the design of composite structures. In particular, new genetic operators are introduced to improve the reliability of the code, on the basis of the investigations conducted by Nagendra et al. [12]. The code is implemented in Matlab language, and can be easily linked to the structural analysis tool described in the previous section. As input data, the optimization routine requires the definition of the number of variables, their range, the cardinality of the alphabet to encode the variables, the functions to compute the fitness and the constraints, the penalty terms associated to each of the constraints, and the parameters relative to the mutation operators.

The optimization process begins with the initial construction of a pool of candidates, i.e. the first generation of individuals. The quality of each of the individuals, i.e. the first set of possible designs, is initially established by evaluation of their fitness function, including the penalty contribution due to the constraints that the design is required to satisfy.

Depending on the fitness of each single individual, the members of the first generation are sorted and submitted to the selection process, which can be based on different criteria. In the present implementation, a probability is attributed to the individuals based on their ranking: the fittest members are those with highest chance of being selected for becoming parents, while the less fit are unlikely to be selected. In any case, a not null probability is associated to all the members of the pool, so that even the less fit designs have a chance of becoming parents. This aspect, together with the other mutation operators, plays an important role in guaranteeing that the optimization process does not converge to local minima.

For each couple of parents, new individuals are created by applying the crossover operator. It consists in recombining the information encoded in the chromosomes of the selected parents to obtain a new design. The single point crossover is here considered among the various implementations proposed in the literature.

The mutation operator is applied just after the application of the crossover. In this case, mutation is performed by means of four different operators. The last step of the genetic process consists in the insertion of the offspring into the new generation. The optimization code allows to define an arbitrary number of elite members. The overall procedure is repeated until a convergence criterion is met. Different criteria are implemented in the code, consisting in the maximum number of generations, fitness functions evaluations and generations with no improvement of the best individuals.

3.1   Chromosome encoding

Genetic algorithms work with populations of designs, where each of the design is identified by a chromosome. Each individual is represented by a chromosome, which is responsible for the encoding of the genetic information. To this aim, different alphabets can be used, the binary representation being one of the most common. In the context of stacking sequence optimization, design variables are represented by the angles of orientation of each ply, and the problem becomes an integer optimization problem (or a mixed-integer problem if, in addition, other real variables are involved). A suitable strategy for the encoding of the angles of orientation of a laminate consists in the use of alphabets of higher cardinality, where an integer number is associated to each ply angle. The cardinality of the alphabet is then dependent on the number of plies made available for the design. For instance, a 3-ary alphabet is considered if the plies can be oriented at 0°, 45°, 90°.

In the present work, alphabets of cardinality of 7 and 13 are considered, in order to allow the design of panels with plies oriented from 0° to 90°, with steps of 15° and 7.5°, respectively. In the first case, the value 0 means 0°, 1 means 15°, 2 stands for 30°, and so on. Furthermore, the pool of available design is restricted to that of balanced laminates. To this aim the chromosome encoding is performed such that each gene denotes a couple of plies oriented at ±θ. This strategy is inspired by the results reported in Ref. [13], where it was demonstrated that a penalty approach is not efficient to enforce the balance constraint, adding noise to the fitness function. An example of chromosome decoding is reported in Eq. (40) assuming the case of cardinality 7:

$$[303441] \rightarrow [\pm 45°/\pm 0°/\pm 45°/\pm 60°/\pm 60°/\pm 15°] \qquad (39)$$

It is remarked that the optimization code implemented allows the introduction of any encoding rule, so that the assumption of balanced laminates, or the use of different alphabets can be easily modified. Laminates with a variable number of plies are handled by associating an integer value to a dummy ply.

3.2   Genetic operators

The crossover operator is here implemented in its one-point version, meaning that one single cut point is randomly chosen for each of the two parents. The crossover operator is slightly modified when a variable number of plies is allowed. In this case, the chromosome is firstly resorted by packing all the N empty plies in the first N genes, and the crossover cut point is forced to fall in the remaining genes.
Regarding the mutation operators, specific operators have been implemented to improve the reliability of the procedure, as demonstrated in Ref. [12].
The first operator is the ply swap, consisting in a random selection and the swap of two plies. The use of this operator is motivated by the fact that inner and outer plies have different influences on the bending stiffness of the laminate. Therefore the external plies reach convergence faster than the internal ones.
A second mutation operator is the angle ply mutation that consists in randomly picking one gene and altering its value with any of the possible angles. In presence of a variable number of plies, two more operators are available, namely the ply addition and ply deletion operators. Their application consists in the addition of a randomly oriented ply, or the deletion of a ply. It is noted that ply addition and deletion operators are applied to the innermost ply, the less influent in terms of laminate bending stiffness. With this approach, abrupt changes of laminate bending stiffness, which may have a too drastic impact on the mutated individual, are avoided.
After crossover and mutation operations, the new generation is created applying an elitist selection. Elitism is a well know strategy to improve the convergence properties of the genetic algorithm. On one hand, it has the effect of speeding-up the convergence to a maximum, but on the other hand it weakens the explorative ability of the method in the design space. In this implementation elitism is implemented by taking the fittest individual. Elite members are passed intact to the following generation in order to guarantee that the fittest individuals are not lost due to the application of the genetic operators during crossover and mutation.
The selection is performed with a tournament with variable size. The effect of enlarging the tournament size is to increase the selective pressure, with the risk of reducing the diversity in the new population. For this reason, a size of 2 is here considered.

4   ANALYTICAL/NUMERICAL COMPARISON

Before illustrating the results of the optimization, the quality of the semi-analytical predictions is assessed by presenting the comparison between analytical and numerical results. The commercial code Abaqus is used for this purpose, and the finite element model is realized by modeling the full representative unit of Figure 1. The four edges of the model are subjected to periodic constraints. In particular, the two transverse edges are forced to undergo equal translations along the z direction and rotations around the x-axis. Furthermore, the edges are forced to remain straight. The longitudinal edges are subjected to a constraint equation forcing the nodal degrees of freedom to display equal translations along z and rotations around y. Regarding the translation along the x direction, the axial load is introduced by defining a constraint equation:

$$u_x^{upper} - u_x^{lower} = \Delta U \qquad (40)$$

where u_x^{upper} and u_x^{lower} are the set of nodes belonging to the upper and lower edges of the panel, respectively, while ΔU is the imposed shortening.

The finite element analyses are conducted by performing a preliminary eigenvalue analysis to determine the bifurcation buckling load. The nonlinear response is studied with a quasi-static nonlinear step, assuming an initial imperfection equal to the first buckling mode with maximum nondimensional amplitude w_0/t of 10%. The mesh is realized using four node S4R elements, with a typical dimension of 5 mm.

Two panels are here considered for comparison purposes. They have equal geometry, but different stacking sequences. The length a is equal to 450 mm, and the width b is 150 mm. The two panels are assumed to be made of the unidirectional material IM7/8552, whose elastic properties are summarized in Table 1.

E_{11} [MPa]	E_{22} [MPa]	G_{12} [MPa]	v_{12}	ρ [kg/m^3]
150000	9080	5290	0.32	1570

Table 1: Material properties of IM7/8552.

The ply thickness is 0.125 mm. As far as the panels are obtained by the stacking of eight plies, the total thickness is 1.0 mm. The lay-ups here considered are:

- Panel 1: [0$_4$/90$_4$]
- Panel 2: [30$_4$/-30$_4$]

Semi-analytical calculations are conducted using 12×12 shape functions, corresponding to a total number of 145 degrees of freedom, obtained as the sum of the 144 unknown amplitudes and the additional unknown due to the load parameter. The buckling loads and the first natural frequency are summarized in Table 2.

	Panel 1		Panel 2	
	P_{buck} [N]	ω [rad/s]	P_{buck} [N]	ω [rad/s]
Abaqus	982.9	607.2	1305.1	470.3
Analytical	979.3	605.6	1315.6	470.9
%diff	-0.37	-0.26	0.80	0.13

Table 2: Comparison of buckling and eigenfrequency analysis for Panels 1 and 2.

The percent differences of Table 2 are below 1%, revealing a good degree of agreement between numerical and analytical results. It is observed that the quality of the results is slightly lower in the case of buckling analysis, probably due to the assumption on null prebuckling deflections introduced in the analytical model.

Postbuckling results are compared in Figure 2 for Panels 1 and 2 in terms of force-shortening curve and maximum out of plane displacement during the loading phase.
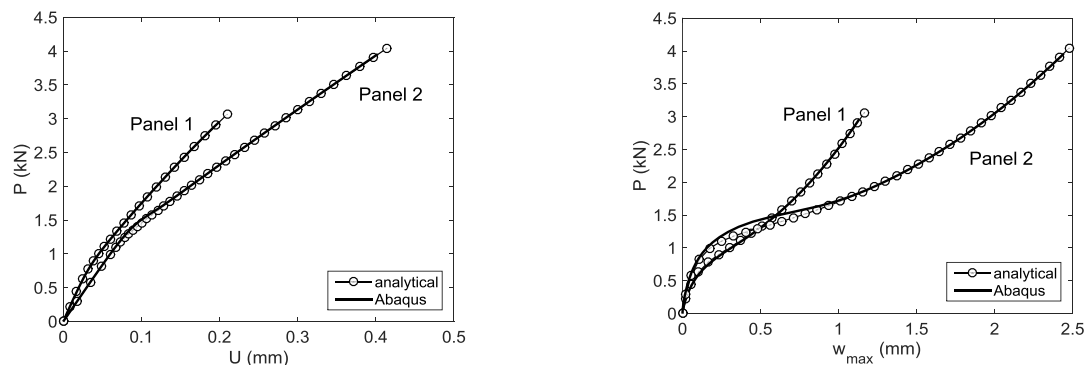

Figure 2: Numerical/analytical comparison for Panels 1 and 2:
(a) force-shortening curve, (b) max out of plane displacement.

The comparison demonstrates the good quality of the analytical predictions, as the curves are almost undistinguishable with those obtained using Abaqus. It is important to remark the time needed to complete the analysis: the average time for the Panels 1 and 2 is approximately 0.9 seconds with the analytical tool, and 130 seconds with Abaqus.

To illustrate the potentialities of the method in capturing also the stress redistribution due to the postbuckling deflections, the comparison is reported in Figure 3 for Panel 2 in terms of axial force per unit length N_{xx} at a load level of $P/P_{buck} = 3.0$.

Figure 3: Contour of N_{xx} for Panel 2 at $P/P_{buck} = 3.0$: (a) analytical, (b) Abaqus.

The results of Figure 3 illustrate similar patterns and a difference below 7% in terms of maximum values. Similar results, with good prediction of the contour pattern and a maximum difference of 6.5%, are obtained for Panel 1.

5   DESIGN OPTIMIZATION USING THE FAST METHOD

To illustrate the potentialities of the fast design procedure, the optimal design of two panels is discussed, introducing requirements on the linear and nonlinear response.

The dimensions of the panel are assumed to be known a priori: the length is fixed to 450 mm and the width is 150 mm. The laminate is layered with a number of 16 plies, whose elastic properties are those of Table 1, and the overall thickness of the laminate is 2 mm. The optimization problem is presented in the form of a stacking optimization problem, where the design variables are the angles of orientation of the plies. The constraint of balanced laminate is enforced a priori by assuming a stacking sequence with plies at $\pm\theta$, thus reducing the total number of design variables to 8. Each ply is allowed to assume an orientation between 0° and 90°. Two possible angle steps are assumed. In a first optimization the plies are allowed to vary with an angle of 15°. The total number of possible designs is equal to 7^8, and the optimal configuration is denoted as Opt15. In a second run, the plies can vary with a step of 7.5°, thus allowing a huge enlargement of the design space to 13^8 combinations (more than 800 million possible designs). In this case, the optimum is denoted as Opt75.

The optimization aims to improve the panel response with respect to a quasi-isotropic baseline with lay-up $[\pm 45/0_2/90_2/0_2]_s$, quantifying the possible benefits due to the adoption of different ply steps.

The optimization problem is formulated as the maximization of the linear buckling load subjected to a constraint regarding the first natural frequency and the maximum out of plane displacement in the postbuckling field. In particular, the problem is formulated as:

$$\begin{aligned}
\max \quad & P_{buck} \\
\text{subject to:} \quad & \begin{cases} \omega > \overline{\omega} \\ w_{max} < \overline{w}_{max} \ \text{ at } P = 2.5 \, \overline{P}_{buck} \end{cases}
\end{aligned} \tag{41}$$

The overline denotes the reference quantities, which are established by analyzing the baseline configuration. In particular, the first natural frequency of vibration is $\overline{\omega} = 1600 \, \text{rad/s}$, while the buckling load is $\overline{P}_{buck} = 23.1 \, \text{kN}$.

The constraint on the maximum out of plane displacement is $\overline{w}_{max} = 3.90 \, \text{mm}$, and is measured at a load level equal 2.5 times the buckling load. This latest condition ensures that, within the design space under investigation, all the panels are required to work in the postbuckling field. Indeed, the solution of the unconstrained buckling maximization problem identifies the configuration with all the plies at $\pm 45°$

as the optimal solution and the corresponding buckling load is $P_{buck} = 27.8$ kN. It is interesting to highlight that the configuration that maximizes the buckling load exhibits a maximum out of plane displacement of 6.98 mm when $P = 2.5\,\overline{P}_{buck}$, therefore violating the nonlinear constraint here imposed.

5.1   Results

The results obtained for the two optimizations are here discussed. The parameters to set up the analysis are the same in both cases, apart from the size of the population, which is equal to 30 individuals when the ply step is 15°, and is 50 when the step is increased 7.5°. The number of élite individuals is fixed to 1, so guaranteeing that the best member of each generation is passed intact to the following generation. Fitness scaling is performed using a rank-based strategy, where the fitness is scaled depending on the rank of each individual instead of its score.

The stopping criterion is based on the maximum number of generations without improvements. The procedure terminates if the weighted average relative change in the best fitness function value over 50 generations is less than or equal to a tolerance set of 1e-8.

The fitness of the best individual of each generation, until convergence, is reported in Figure 4.
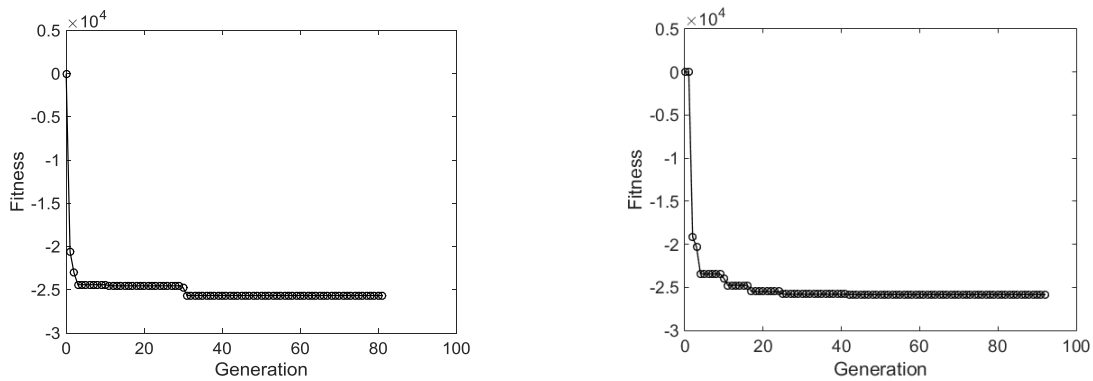

Figure 4: Fitness function versus generation: (a) Opt15, (b) Opt75.

The first optimization terminates after 81 generations, while the second one requires a total of 92 generations to meet the stopping criterion. Considering the numbers of individuals used in the two cases, the overall number of function evaluations is equal to 2430 for the first run and 4600 for the second one. In any case, a reduced computational effort is guaranteed in both cases, thanks to the efficient implementation of the analysis tool. All the analysis are performed on Core i7 2.30 GHz laptop, with 16 GB of RAM. The computational time to perform the two optimizations is approximately 39 and 77 minutes, respectively.

The two optimal configurations and the corresponding values of buckling load, first natural frequency and maximum out of plane displacement are summarized in Table 3.

	Layup	P_{buck} [kN]	ω [rad/s]	w_{max} [mm]
Ref. values	$[\pm45/0_2/90_2/0_2]_s$	23.1	1600	3.87
Opt15	$[\pm60/\pm45/\pm30/\pm0_2/\pm30/\pm45/\pm60]$	25.6	1913	3.90
Opt75	$[\pm52.5/\pm60/\pm22.5/\pm7.5_2/\pm30/\pm60/\pm52.5]$	25.8	1909	3.78

Table 3: Results of the optimization.

As observed from Table 3, the two optimal solutions satisfy the design constraints and allow an increase of the panel buckling load. The Opt15 is characterized by a buckling load 10.8% higher compared to the baseline. On the other hand, no significant improvement is achieved by enlarging the design space as in the case of the Opt75 design. In this case, the buckling load is 11.7% higher than the baseline, but still very close to the Opt15 configuration.

6   CONCLUSIONS

The development of a semi-analytical procedure with postbuckling capabilities has been discussed together with its implementation in the context of an optimization toolbox based on genetic algorithms. The main advantage of the approach is the possibility of considering a wide class of laminates, including those characterized by midplane unsymmetry, in a very efficient manner. The comparison with Abaqus simulations allowed to conclude that the method combines the rapidity typical of closed-form solutions with the accuracy of finite element analyses. As a result, the method is particularly suitable to perform structural optimizations, even when large design spaces are of concern. In this sense, the proposed optimization toolbox can successfully be employed to fully exploit the tailoring opportunities offered by composite materials, making possible the design of structures characterized by unconventional layups. Two applicative examples have been discussed regarding the buckling maximization of panels layered with 16 plies and ply angles oriented with steps of 7.5° and 15°. The results have illustrated the possibility of improving the buckling load of the structure while restricting its postbuckling deflections at a given load level. No significant improvement was observed by enlarging the design space from ply steps of 15° to 7.5°, but general conclusions cannot be drawn as loading conditions were restricted to the case of pure compression. The benefits of considering ply steps of 7.5° could be more relevant if more complex loading conditions are investigated. In this sense, further investigation is still needed.

7   ACKNOWLEDGEMENTS

8   REFERENCES

[1]   C. Bisagni and R. Vescovini, "Analytical formulation for local buckling and post-buckling analysis of stiffened laminated panels," *Thin-Walled Structures,* **47**, 2009, pp. 318-334.

[2]   C. Bisagni and R. Vescovini, "Fast tool for buckling analysis and optimization of isotropic and composite stiffened panels," *Journal of Aircraft,* **46**, 2009, pp. 2041-2053.

[3]   R. Vescovini and C. Bisagni, "Buckling analysis and optimization of stiffened composite flat and curved panels," *AIAA Journal,* **50**, 2012, pp. 904-915.

[4]   R. Chandra, "Postbuckling analysis of crossply laminated plates," *AIAA Journal,* **13**, 1975, pp. 1388-1389.

[5]   M.-L. Dano and M.W. Hyer, "Thermally-induced deformation behavior of unsymmetric laminates," *International Journal of Solids and Structures,* **35**, 1998, pp. 2101-2120.

[6]   C.G. Diaconu and P.M. Weaver, "Postbuckling of long unsymmetrically laminated composite plates under axial compression," *International Journal of Solids and Structures,* **43**, 2006, pp. 6978-6997.

[7]   K. Nie, Y. Liu, and Y. Dai, "Closed-form solution for the postbuckling behavior of long unsymmetrical rotationally-restrained laminated composite plates under inplane shear," *Composite Structures,* **122**, 2015, pp. 31-40.

[8]   Y. Zhang and F.L. Matthews, "Postbuckling behaviour of curved panels of generally layered composite materials," *Composite Structures,* **1**, 1983, pp. 115-135.

[9]   J. Zhang, Q. Li, and Y. Shu, "Nonlinear stability of unsymmetrically laminated angle-ply shear-deformable plates in biaxial compression," *Thin-Walled Structures,* **38**, 2000, pp. 1-16.

[10]   R. Vescovini and C. Bisagni, "Two-step procedure for fast post-buckling analysis of composite stiffened panels," *Computers & Structures,* **128**, 2013, pp. 38-47.

[11]   E. Byklum and J. Amdahl, "A simplified method for elastic large deflection analysis of plates and stiffened panels due to local buckling," *Thin-Walled Structures,* **40**, 2002, pp. 925-953.

[12]   S. Nagendra, D. Jestin, Z. Gürdal, R.T. Haftka, and L.T. Watson, "Improved genetic algorithm for the design of stiffened composite panels," *Computers & Structures,* **58**, 1996, pp. 543-555.

[13]   L. Grosset, S. Venkataraman, and R.T. Haftka, "Genetic optimization of two-material composite laminates," in *16th ACS Conference*, Blacksburg, Virginia, 2001.